

## Instability of the ion hybrid wave in the presence of superthermal alpha-particles

C. N. Lashmore-Davies and D. A. Russell

Citation: *Phys. Plasmas* **4**, 369 (1997); doi: 10.1063/1.872096

View online: <http://dx.doi.org/10.1063/1.872096>

View Table of Contents: <http://pop.aip.org/resource/1/PHPAEN/v4/i2>

Published by the [American Institute of Physics](#).

---

### Related Articles

Time growth rate and field profiles of hybrid modes excited by a relativistic elliptical electron beam in an elliptical metallic waveguide with dielectric rod  
*Phys. Plasmas* **19**, 102110 (2012)

Toroidal rotation of multiple species of ions in tokamak plasma driven by lower-hybrid-waves  
*Phys. Plasmas* **19**, 102505 (2012)

Wave breaking phenomenon of lower-hybrid oscillations induced by a background inhomogeneous magnetic field  
*Phys. Plasmas* **19**, 102302 (2012)

Measurements of ion cyclotron range of frequencies mode converted wave intensity with phase contrast imaging in Alcator C-Mod and comparison with full-wave simulations  
*Phys. Plasmas* **19**, 082508 (2012)

Backward mode of the ion-cyclotron wave in a semi-bounded magnetized Lorentzian plasma  
*Phys. Plasmas* **19**, 082101 (2012)

---

### Additional information on Phys. Plasmas

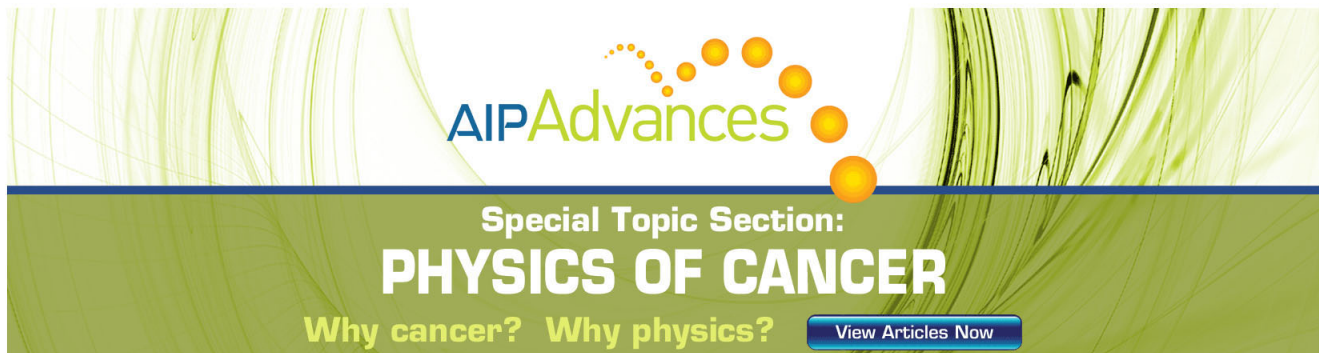
Journal Homepage: <http://pop.aip.org/>

Journal Information: [http://pop.aip.org/about/about\\_the\\_journal](http://pop.aip.org/about/about_the_journal)

Top downloads: [http://pop.aip.org/features/most\\_downloaded](http://pop.aip.org/features/most_downloaded)

Information for Authors: <http://pop.aip.org/authors>

## ADVERTISEMENT



**AIP Advances**

Special Topic Section:  
**PHYSICS OF CANCER**

Why cancer? Why physics? [View Articles Now](#)

# Instability of the ion hybrid wave in the presence of superthermal alpha-particles

C. N. Lashmore-Davies

UKAEA, Fusion (UKAEA/Euratom Fusion Association), Culham, Abingdon, Oxon, OX14 3DB, United Kingdom

D. A. Russell

Lodestar Research Corporation, Boulder, Colorado 80301

(Received 26 June 1996; accepted 4 November 1996)

The stability of the ion hybrid wave in a plasma containing two thermal ion species present in comparable proportions and a low density population of superthermal alpha-particles is analyzed. A simple, model distribution function consisting of a ring distribution in the perpendicular velocity and a Maxwellian in the parallel velocity is used for the superthermal alpha-particles. This distribution function is relevant to the core plasma of a tokamak in the immediate post-birth phase before the alpha-particles have had time to relax collisionally and is therefore of interest to the alpha-channelling question. It has also been used to interpret ion cyclotron emission from fusion products in the edge plasma of large tokamaks. An approximate dispersion relation is derived which allows the conditions for instability to be explored and an analytic expression for the growth rate to be obtained. It is found that the ion hybrid wave can be unstable for  $v_{\perp 0}/c_A \ll 1$  where  $v_{\perp 0}$  is the alpha-particle ring speed and  $c_A$  is Alfvén speed for a plasma with two ion species. The instability conditions obtained from the analytic approximation are used to guide the solution of the exact dispersion relation. Numerical solutions for the specific cases of deuterium–tritium core and edge plasmas in the Tokamak Fusion Test Reactor (TFTR) [K. M. Young *et al.*, Plasma Phys. Controlled Fusion **26**, 11 (1984)] are given. [S1070-664X(97)02602-5]

## I. INTRODUCTION

The existence of the ion hybrid resonance was first pointed out by Buchsbaum<sup>1</sup> in 1960. This resonance, which is a property of a magnetized plasma with more than one ion species, plays a very important role in ion cyclotron heating schemes. The ion hybrid resonance of a two ion species plasma gives rise to an additional member of the family of ion Bernstein waves which, unlike all other ion Bernstein waves, does not have its cut-off frequency at a harmonic of the ion cyclotron frequency of one of the ion species. The cut-off occurs at the ion hybrid frequency which lies between the two cyclotron frequencies. For this reason it has been suggested<sup>2</sup> that this special wave be given its own name, the ion hybrid wave. We shall adopt this nomenclature in the present paper. It is worth observing that the cold ion hybrid resonance of a two ion species plasma turns out to be the cut-off frequency for a propagating wave in a hot, two ion species plasma.

The ion hybrid wave in a plasma with two or more ion species present with comparable concentrations has recently been under very active investigation. This is because, under these conditions, there can be very efficient mode conversion of the fast Alfvén wave to the ion hybrid wave in the vicinity of the ion hybrid resonance. Furthermore, because of the large ion concentrations the ion cyclotron resonances are well separated from the ion hybrid resonance so that ion cyclotron damping is negligible in the region of the hybrid resonance. The only collisionless damping suffered by the ion hybrid wave, near the hybrid resonance, is due to the electrons. This, of course, refers explicitly to the case of approximately equal ion concentrations. The comparable ion

concentrations scheme has been studied by Majeski *et al.*<sup>3</sup> who first suggested that efficient mode conversion could occur when the fast wave is incident from the low field side and demonstrated experimentally on the Tokamak Fusion Test Reactor (TFTR)<sup>4</sup> that, indeed, strong electron heating was produced.

Because the ion hybrid wave is capable of excitation by these means and because the location of the mode conversion is governed by the position of the ion hybrid resonance, the ion hybrid wave was suggested<sup>5</sup> as a promising candidate for the alpha-channelling scheme proposed by Fisch.<sup>6</sup> In this scheme a suitable wave is required to interact with the centrally born fusion alpha-particles before they have had time to slow down. The free energy of the superthermal alpha-particles amplifies the wave which eventually deposits the energy gained into the thermal particles, either ions or electrons. This is only part of the alpha-channelling scheme but it provides a motivation to investigate the stability of the ion hybrid wave in the presence of superthermal alpha-particles.

In order to gain insight into the conditions required for instability we have considered a simple model for the superthermal alpha-particle distribution. The model we have chosen consists of a ring distribution in perpendicular velocity and a Maxwellian for the parallel velocity with a high parallel temperature. Such a distribution has been shown to be relevant to ion cyclotron emission<sup>7,8</sup> from fusion products in the edge plasmas of the Joint European Torus<sup>9</sup> (JET) and TFTR. Although rather idealized, this distribution possesses the key ingredients of the immediate post-birth alpha-particle distribution, namely free perpendicular energy and a large spread of parallel velocities. The use of this simple distribu-

tion is justified by the fact that the still very complicated dispersion relation is, nevertheless, analytically tractable, thus permitting the extraction of a number of important scalings and other aids to an understanding of the physics of this problem.

The stability analysis of the ion hybrid wave in the presence of superthermal (fusion) alpha-particles may also be relevant to the ion cyclotron emission (ICE) observations from TFTR. This is because for most conditions under which ICE is observed, the alpha-particles are sub-Alfvénic. The favored emission mechanism,<sup>8</sup> which involves the fast Alfvén wave, whilst still operative, is less unstable under these conditions. However, since the ion hybrid wave is a slow wave the Alfvén speed is of no significance and we may expect the wave to be unstable independently of whether the ring speed,  $v_{\perp 0}$ , is above or below the Alfvén speed  $c_A$ .

The plan of the paper is as follows. In Sec. II we present the exact electromagnetic dispersion relation for a hot, uniform plasma containing two thermal ion species and a low concentration of superthermal alpha-particles. The emphasis is on the case where the two thermal ion species have comparable concentrations, for which an approximate dispersion relation is derived. In Sec. III the conditions for instability of the ion hybrid wave are discussed and the approximate dispersion relation is solved analytically for the growth rate. Numerical solutions for the frequency and growth rate of the exact dispersion relation are given in Sec. IV and a summary and conclusions are given in Sec. V.

## II. THE DISPERSION RELATION

The ion hybrid wave is a member of the family of ion Bernstein waves. Since it originates from the cold plasma resonance, characteristic of a two ion species plasma, it is logical to refer to it as the ion hybrid wave<sup>2</sup> by analogy with its two higher frequency counterparts, the lower hybrid wave and the upper hybrid wave. The ion hybrid wave is also distinguished amongst the ion Bernstein waves as being the only one whose cut-off frequency does not occur at a multiple of an ion cyclotron frequency. In order to analyze the stability of the ion hybrid wave in the presence of a population of superthermal ions it will be necessary to consider the main damping mechanisms for this wave.

A case of particular interest is when the two ion species are present in comparable proportions. Under these conditions, the ion hybrid wave for long wavelengths has a frequency which is well separated from the two ion cyclotron frequencies and therefore will not be subject to ion cyclotron damping even for significant values of the parallel wave number. Because the ion hybrid wave can couple to the fast Alfvén wave and because it is susceptible to collisionless electron dissipation (electron Landau and transit time damping) a quantitative description of the ion hybrid wave requires the full, electromagnetic dispersion relation. We consider the idealized model of a uniform plasma with the magnetic field in the  $z$ -direction and waves with harmonic space and time dependence,  $\exp(i(\mathbf{k} \cdot \mathbf{x} - \omega t))$  where  $\mathbf{k} = (k_{\perp}, 0, k_{\parallel})$ . The dispersion relation can be written<sup>8</sup> as

$$\begin{aligned} & (n_{\perp}^2 - \varepsilon_{zz}) \{ (n_{\parallel}^2 - \varepsilon_{xx})(n_{\perp}^2 - \varepsilon_{yy}) + \varepsilon_{xy}^2 + (n_{\parallel}^2 - \varepsilon_{xx})n_{\perp}^2 \} \\ & - (n_{\parallel}^2 - \varepsilon_{yy})n_{\parallel}^2 n_{\perp}^2 - n_{\parallel}^2 n_{\perp}^4 = \varepsilon_{yz} \{ \varepsilon_{xy}(n_{\perp} n_{\parallel} + \varepsilon_{xz}) \\ & - \varepsilon_{yz}(n_{\parallel}^2 - \varepsilon_{xx}) \} + \varepsilon_{xz} \{ \varepsilon_{xy} \varepsilon_{yz} + (n_{\perp} n_{\parallel} + \varepsilon_{xz})(n_{\perp}^2 - \varepsilon_{yy}) \} \\ & + n_{\parallel} n_{\perp} \{ \varepsilon_{xy} \varepsilon_{yz} + \varepsilon_{xz}(n_{\perp}^2 - \varepsilon_{yy}) \}, \end{aligned} \quad (1)$$

where  $n_{\parallel} = ck_{\parallel}/\omega$ ,  $n_{\perp} = ck_{\perp}/\omega$  and  $n^2 = n_{\perp}^2 + n_{\parallel}^2$ . Solutions to Eq. (1) will be presented in Sec. IV. In order to gain some insight into the problem we introduce approximations to Eq. (1). First we note<sup>10</sup> that Eq. (1) has been written in a form in which the right-hand-side disappears as the temperature tends to zero. The right-hand-side is small provided  $(v_{Ti} n_{\parallel}/c)^2 \ll 1$ , where  $v_{Ti}$  is the ion thermal speed, a condition which is well satisfied in present tokamaks. Furthermore, for the ion cyclotron range of frequencies  $\varepsilon_{zz}$  is the dominant element of the dielectric tensor. Keeping only the terms on the left-hand-side of Eq. (1) which are proportional to  $\varepsilon_{zz}$  and retaining only those terms on the right-hand-side (as a perturbation) which contribute to the collisionless electron absorption, Eq. (1) is reduced to the form

$$\begin{aligned} & n_{\perp}^2 (\varepsilon_{xx} - n_{\parallel}^2) - (\varepsilon_{yy}^i - n_{\parallel}^2)(\varepsilon_{xx} - n_{\parallel}^2) - \varepsilon_{yz}^2 \\ & \simeq \left( \frac{\varepsilon_{yz}^2}{\varepsilon_{zz}} + \varepsilon_{yy}^e \right) (\varepsilon_{xx} - n_{\parallel}^2) + \frac{n_{\parallel}^2 n_{\perp}^4}{\varepsilon_{zz}}. \end{aligned} \quad (2)$$

Notice that the  $\varepsilon_{yy}$  element has been separated into its ion and electron parts  $\varepsilon_{yy}^i$  and  $\varepsilon_{yy}^e$ , respectively, and the electron contribution, which describes transit time damping, has been transferred to the right-hand-side of Eq. (2). The physical significance of Eq. (2) is the following. If the right-hand-side is neglected, the left-hand-side, for  $\mu_0 n_{0e} T_i / B_0^2 > m_e / m_i$ , describes fast compressional Alfvén waves and ion Bernstein waves for which the parallel electric field has been neglected<sup>2</sup> ( $n_{0e}$  is the equilibrium electron density,  $\mu_0$  the magnetic permeability of free space,  $T_i$  the temperature of the thermal ions and  $B_0$  the equilibrium magnetic field). Taking account of the right-hand-side includes the effect of the parallel electric field and all the collisionless electron dissipative mechanisms. The first term on the right-hand-side of Eq. (2) is responsible for the electron damping of the fast Alfvén wave which arises from a combination of electron Landau and transit time dissipation. The decay of the ion hybrid wave is due to electron Landau damping which is dominated by the last term on the right-hand-side of Eq. (2).<sup>11</sup>

In the general case the hot plasma expressions for the dielectric tensor elements on the left-hand-side should be used. In this way the effect of ion cyclotron damping is introduced. However, in the present analytic treatment we take advantage of the separation of the two-ion hybrid resonance frequency from the ion cyclotron frequencies. Under these circumstances the thermal ion terms can be represented by their cold plasma approximations in Eq. (2). Since  $\varepsilon_{xx} = \varepsilon_{yy}^i = \varepsilon_{\perp}$ , we write Eq. (2) as

$$\begin{aligned} & (\varepsilon_{\perp} - n_{\parallel}^2)n_{\perp}^2 - (\varepsilon_{\perp} + i\varepsilon_{xy} - n_{\parallel}^2)(\varepsilon_{\perp} - i\varepsilon_{xy} - n_{\parallel}^2) \\ & \simeq -\varepsilon_{xx}^{\alpha} n_{\perp}^2 + (\varepsilon_{\perp} - n_{\parallel}^2) \varepsilon_{xx}^{\alpha} + (\varepsilon_{\perp} - n_{\parallel}^2) \varepsilon_{yy}^{\alpha} + 2\varepsilon_{xy} \varepsilon_{xy}^{\alpha}, \end{aligned} \quad (3)$$

where we have neglected the damping terms on the right-hand-side of Eq. (2) for the moment but will consider their effect later. The terms on the left-hand-side of Eq. (3) are all due to the thermal species of the plasma. The terms on the right-hand-side of Eq. (3),  $\varepsilon_{ij}^\alpha$ , are due to the fusion alpha-particles but, in general, could represent any small population of superthermal ions. The alpha-particle terms are treated perturbatively and only those terms linear in the alpha-particle density have been retained. For two, arbitrary ion species, labelled 1 and 2, we have

$$\varepsilon_\perp \approx -\frac{\omega_{p1}^2}{(\omega^2 - \Omega_1^2)} - \frac{\omega_{p2}^2}{\omega^2 - \Omega_2^2}, \quad (4)$$

$$\varepsilon_{xy} \approx -\frac{i\omega_{p1}^2\omega}{(\omega^2 - \Omega_1^2)\Omega_1} - \frac{i\omega_{p2}^2\omega}{(\omega^2 - \Omega_2^2)\Omega_2}, \quad (5)$$

where  $\omega_{pj}$ ,  $\Omega_j$  are the plasma and cyclotron frequencies of the  $j$ -th ion species, respectively, and the vacuum and electron contributions to  $\varepsilon_\perp$  have been neglected but the electron contribution to  $\varepsilon_{xy}$  is included. Using Eqs. (4) and (5) we obtain

$$\varepsilon_\perp + i\varepsilon_{xy} = \frac{\omega_{p1}^2}{\Omega_1(\omega + \Omega_1)} + \frac{\omega_{p2}^2}{\Omega_2(\omega + \Omega_2)}, \quad (6)$$

$$\varepsilon_\perp - i\varepsilon_{xy} = -\frac{\omega_{p1}^2}{\Omega_1(\omega - \Omega_1)} - \frac{\omega_{p2}^2}{\Omega_2(\omega - \Omega_2)}. \quad (7)$$

Substituting Eqs. (4), (6) and (7) into the left-hand-side of Eq. (3) and multiplying through the equation by  $(\Omega_1^4/\omega_{p1}^4)(\Omega_1^2 - \omega^2)(\omega^2 - \Omega_2^2)(\omega^2/\Omega_1^2)$  we obtain

$$c_{A1}^2 k_\perp^2 \left( 1 + \frac{\omega_{p2}^2}{\omega_{p1}^2} \right) \left\{ \frac{\omega^2 - \Omega_{ii}^2 + \frac{c_{A1}^2 k_\parallel^2}{\omega^2} \left( \frac{\omega^2}{\Omega_1^2} - 1 \right) (\omega^2 - \Omega_2^2)}{\left( 1 + \frac{\omega_{p2}^2}{\omega_{p1}^2} \right)} \right\}$$

$$\begin{aligned} & -\omega^2 \left\{ \omega - \Omega_1 + \frac{\omega_{p2}^2}{\omega_{p1}^2} \frac{\Omega_1}{\Omega_2} \frac{(\omega^2 - \Omega_1^2)}{(\omega + \Omega_2)} - \frac{c_{A1}^2 k_\parallel^2}{\omega^2 \Omega_1} (\omega^2 - \Omega_1^2) \right\} \\ & \times \left\{ \frac{(\omega^2 - \Omega_2^2)}{(\omega - \Omega_1)} + \frac{\omega_{p2}^2}{\omega_{p1}^2} \frac{\Omega_1}{\Omega_2} (\omega + \Omega_2) + \frac{c_{A1}^2 k_\parallel^2}{\omega^2 \Omega_1} (\omega^2 - \Omega_2^2) \right\} \\ & = \frac{\Omega_1^4}{\omega_{p1}^4} (\omega^2 - \Omega_1^2) (\omega^2 - \Omega_2^2) \frac{\omega^2}{\Omega_1^2} \\ & \times \{ \varepsilon_{xx}^\alpha n_\perp^2 - (\varepsilon_\perp - n_\parallel^2) \varepsilon_{xx}^\alpha - (\varepsilon_\perp - n_\parallel^2) \varepsilon_{yy}^\alpha - 2\varepsilon_{xy}^\alpha \varepsilon_{xy} \}; \end{aligned} \quad (8)$$

where  $c_{A1}^2$  is the square of the Alfvén speed associated with species 1 ( $B_0^2/\mu_0\rho_1$ ) where  $\rho_1 \equiv n_1 m_1$  is the mass density of ion species 1 and

$$\Omega_{ii}^2 = \frac{(\Omega_2^2 \omega_{p1}^2 + \Omega_1^2 \omega_{p2}^2)}{(\omega_{p1}^2 + \omega_{p2}^2)}$$

is the square of the two-ion hybrid resonance frequency.

Since we are considering a plasma with two thermal ion species present in approximately equal proportions it is clear that the fast Alfvén wave will be supported by both ion species which must therefore be treated on an equal footing, in contrast to the more usual minority ion case. With this in mind, Eq. (8) is divided throughout by

$$\left( 1 + \frac{\omega_{p2}^2}{\omega_{p1}^2} \right) \left( 1 + \frac{\rho_2}{\rho_1} \right),$$

where  $\rho_2$  is the mass density of ion species 2 to obtain

$$\begin{aligned} & \frac{c_{A1}^2 k_\perp^2}{\left( 1 + \frac{\rho_2}{\rho_1} \right)} \left\{ \frac{\omega^2 - \Omega_{ii}^2 + \frac{c_{A1}^2 k_\parallel^2}{\omega^2} \left( \frac{\omega^2}{\Omega_1^2} - 1 \right) (\omega^2 - \Omega_2^2)}{\left( 1 + \frac{\omega_{p2}^2}{\omega_{p1}^2} \right)} \right\} - \frac{\omega^2}{\left( 1 + \frac{\omega_{p2}^2}{\omega_{p1}^2} \right) \left( 1 + \frac{\rho_2}{\rho_1} \right)} \left\{ \omega^2 - \Omega_2^2 + \frac{2\omega_{p2}^2}{\omega_{p1}^2} \frac{\Omega_1}{\Omega_2} (\omega^2 - \Omega_1 \Omega_2) \right. \\ & \left. + \frac{\omega_{p2}^4}{\omega_{p1}^4} \frac{\Omega_1^2}{\Omega_2^2} (\omega^2 - \Omega_1^2) - \frac{2c_{A1}^2 k_\parallel^2}{\omega^2} (\omega^2 - \Omega_2^2) - \frac{2c_{A1}^2 k_\parallel^2 \omega_{p2}^2}{\omega^2 \omega_{p1}^2} (\omega^2 - \Omega_1^2) - \frac{c_{A1}^4 k_\parallel^4}{\omega^4 \Omega_1^2} (\omega^2 - \Omega_1^2) (\omega^2 - \Omega_2^2) \right\} \\ & = \frac{\Omega_1^4}{\omega_{p1}^4} (\omega^2 - \Omega_1^2) (\omega^2 - \Omega_2^2) \frac{\omega^2}{\left( 1 + \frac{\omega_{p2}^2}{\omega_{p1}^2} \right) \left( 1 + \frac{\rho_2}{\rho_1} \right)} \Omega_1^2 \{ \varepsilon_{xx}^\alpha n_\perp^2 - (\varepsilon_\perp - n_\parallel^2) \varepsilon_{xx}^\alpha - (\varepsilon_\perp - n_\parallel^2) \varepsilon_{yy}^\alpha - 2\varepsilon_{xy}^\alpha \varepsilon_{xy} \}. \end{aligned} \quad (9)$$

We can now introduce the Alfvén speed defined in terms of the two-ion species, into Eq. (10) and subsequent equations, through the relation

$$c_A^2 \equiv \frac{B_0^2}{\mu_0(\rho_1 + \rho_2)} = \frac{c_{A1}^2}{\left( 1 + \frac{\rho_2}{\rho_1} \right)}. \quad (10)$$

Equation (9) therefore becomes

$$\begin{aligned}
& (\omega^2 - c_A^2 k_\perp^2) \left\{ \omega^2 - \Omega_{ii}^2 + \frac{N_{\parallel}^2 \left( \frac{\omega^2}{\Omega_1^2} - 1 \right) (\omega^2 - \Omega_2^2) \left( 1 + \frac{\rho_2}{\rho_1} \right)}{\left( 1 + \frac{\omega_{p2}^2}{\omega_{p1}^2} \right)} \right\} - \frac{\omega^2}{\left( 1 + \frac{\omega_{p2}^2}{\omega_{p1}^2} \right)} \left\{ \frac{\omega_{p2}^2}{\omega_{p1}^2} \left( \frac{\Omega_1}{\Omega_2} - 1 \right)^2 \frac{\omega^2}{\left( 1 + \frac{\rho_2}{\rho_1} \right)} + 2N_{\parallel}^2 (\omega^2 - \Omega_2^2) \right. \\
& \left. + 2N_{\parallel}^2 \frac{\omega_{p2}^2}{\omega_{p1}^2} (\omega^2 - \Omega_1^2) + \frac{N_{\parallel}^4}{\Omega_1^2} (\omega^2 - \Omega_1^2) (\omega^2 - \Omega_2^2) \left( 1 + \frac{\rho_2}{\rho_1} \right) + N_{\parallel}^2 \left( \frac{\omega^2}{\Omega_1^2} - 1 \right) (\omega^2 - \Omega_2^2) \left( 1 + \frac{\rho_2}{\rho_1} \right) \right\} \\
& = \frac{\Omega_1^4}{\omega_{p1}^4} \frac{(\omega^2 - \Omega_1^2)(\omega^2 - \Omega_2^2)}{\left( 1 + \frac{\omega_{p2}^2}{\omega_{p1}^2} \right) \left( 1 + \frac{\rho_2}{\rho_1} \right)} \frac{\omega^2}{\Omega_1^2} \{ -\varepsilon_{xx}^\alpha n_\perp^2 + (\varepsilon_\perp - n_\parallel^2) \varepsilon_{xx}^\alpha + (\varepsilon_\perp - n_\parallel^2) \varepsilon_{yy}^\alpha + 2\varepsilon_{xy} \varepsilon_{xy}^\alpha \}, \tag{11}
\end{aligned}$$

where  $N_{\parallel}^2 = c_A^2 k_{\parallel}^2 / \omega^2$ .

In order to calculate an explicit dispersion relation we must specify the distribution function of the superthermal ions. We choose the following model distribution which is analytically tractable and possesses the main features relevant to the problem,

$$\begin{aligned}
f_{0\alpha} &= (2\pi^{3/2} v_{\perp 0} v_{T\parallel\alpha})^{-1} \exp\{-(v_{\parallel} - v_d)^2 / v_{T\parallel\alpha}^2\} \\
&\quad \times \delta(v_{\perp} - v_{\perp 0}). \tag{12}
\end{aligned}$$

For the alpha-channelling application it is more appropriate to take the parallel drift velocity  $v_d=0$  and for the immediate post-birth phase an isotropic shell is often used. However, Eq. (12) allows the effects of anisotropy to be included, which may develop subsequently, and incorporates the two key ingredients of the fusion alpha-particles, namely free perpendicular energy characterized by  $v_{\perp 0}$  and a significant spread  $v_{T\parallel\alpha}$  of parallel velocities. The distribution function given by Eq. (12) has previously been used to interpret ion cyclotron emission from the edge plasma in JET and TFTR.<sup>7,8</sup>

Referring to Eq. (11) it can be seen that the following energetic ion, dielectric tensor elements are required:

$$\begin{aligned}
\varepsilon_{xx}^\alpha &= \frac{\omega_{p\alpha}^2}{\omega^2} \left\{ \left[ -1 + \frac{\Omega_\alpha}{k_{\parallel} v_{T\parallel\alpha}} Z(\zeta_{1\alpha}) \right] R \right. \\
&\quad \left. + [1 + \zeta_{1\alpha} Z(\zeta_{1\alpha})] \frac{2v_{\perp 0}^2}{v_{T\parallel\alpha}^2} \frac{J_1^2}{z_\alpha^2} \right\}, \tag{13}
\end{aligned}$$

where

$$R = \frac{2}{z_\alpha} J_1 J_1', \tag{14}$$

$$\zeta_{1\alpha} = (\omega - k_{\parallel} v_d - \Omega_\alpha) / (k_{\parallel} v_{T\parallel\alpha}), \tag{15}$$

and  $z_\alpha = k_{\perp} v_{\perp 0} / \Omega_\alpha$  is the argument of  $J_1$ , the first order Bessel function and its derivative  $J_1'$ ,

$$\begin{aligned}
\varepsilon_{yy}^\alpha &= \frac{\omega_{p\alpha}^2}{\omega^2} \left\{ \left[ -1 + \frac{\Omega_\alpha}{k_{\parallel} v_{T\parallel\alpha}} Z(\zeta_{1\alpha}) \right] P \right. \\
&\quad \left. + [1 + \zeta_{1\alpha} Z(\zeta_{1\alpha})] \frac{2v_{\perp 0}^2}{v_{T\parallel\alpha}^2} J_1'^2 \right\}, \tag{16}
\end{aligned}$$

where

$$P = \frac{2}{z_\alpha} (1 - z_\alpha^2) J_1 J_1', \tag{17}$$

$$\begin{aligned}
\varepsilon_{xy}^\alpha &= \frac{i\omega_{p\alpha}^2}{\omega^2} \left\{ \left[ -1 + \frac{\Omega_\alpha}{k_{\parallel} v_{T\parallel\alpha}} Z(\zeta_{1\alpha}) \right] Q \right. \\
&\quad \left. + [1 + \zeta_{1\alpha} Z(\zeta_{1\alpha})] \frac{2v_{\perp 0}^2}{v_{T\parallel\alpha}^2 z_\alpha} J_1 J_1' \right\}, \tag{18}
\end{aligned}$$

$$Q = J_1'^2 + \left( \frac{1}{z_\alpha^2} - 1 \right) J_1^2. \tag{19}$$

The above dielectric tensor elements are easily obtained, e.g. by substitution of Eq. (13) into Eq. (48), Chap. 10 of Stix.<sup>12</sup> In this paper, the superscript “ $\alpha$ ” refers to alpha-particles but of course may be taken as any energetic ion species, described by the form given in Eq. (12).

The final form of the approximate dispersion relation can be obtained by substituting Eqs. (13), (16) and (18) into Eq. (11) giving

$$\begin{aligned}
& (\omega^2 - c_A^2 k_\perp^2) \left[ \omega^2 - \Omega_{ii}^2 + \frac{N_\parallel^2 \left( \frac{\omega^2}{\Omega_1^2} - 1 \right) (\omega^2 - \Omega_2^2) \left( 1 + \frac{\rho_2}{\rho_1} \right)}{\left( 1 + \frac{\omega_{p2}^2}{\omega_{p1}^2} \right)} \right] - \frac{\omega^2}{\left( 1 + \frac{\omega_{p2}^2}{\omega_{p1}^2} \right)} \left[ \frac{\omega_{p2}^2 (\Omega_1 - \Omega_2)^2 \omega^2}{\omega_{p1}^2 \left( 1 + \frac{\rho_2}{\rho_1} \right) \Omega_2^2} \right. \\
& \left. + 2N_\parallel^2 (\omega^2 - \Omega_2^2) + 2N_\parallel^2 \frac{\omega_{p2}^2}{\omega_{p1}^2} (\omega^2 - \Omega_1^2) + \frac{N_\parallel^4}{\Omega_1^2} (\omega^2 - \Omega_1^2) (\omega^2 - \Omega_2^2) \left( 1 + \frac{\rho_2}{\rho_1} \right) + N_\parallel^2 \left( \frac{\omega^2}{\Omega_1^2} - 1 \right) (\omega^2 - \Omega_2^2) \left( 1 + \frac{\rho_2}{\rho_1} \right) \right] \\
& = - \frac{\omega_{p\alpha}^2}{(\omega_{p1}^2 + \omega_{p2}^2)} (\omega^2 - \Omega_1^2) (\omega^2 - \Omega_2^2) \left\{ \left[ -1 + \frac{\Omega_\alpha}{k_\parallel v_{T\parallel\alpha}} Z(\zeta_{1\alpha}) \right] \left[ N_\perp^2 R + \frac{\Omega_1^2}{(\omega^2 - \Omega_1^2)} \frac{\left( R + P - 2 \frac{\omega}{\Omega_1} Q \right)}{\left( 1 + \rho_2 / \rho_1 \right)} \right. \right. \\
& \left. \left. + \frac{\omega_{p2}^2}{\omega_{p1}^2} \frac{\Omega_1^2}{(\omega^2 - \Omega_2^2)} \frac{\left( R + P - 2 \frac{\omega}{\Omega_2} Q \right)}{\left( 1 + \frac{\rho_2}{\rho_1} \right)} + N_\parallel^2 (R + P) \right] + [1 + \zeta_{1\alpha} Z(\zeta_{1\alpha})] \frac{2v_{\perp 0}^2}{v_{T\parallel\alpha}^2} \left[ N_\perp^2 \frac{J_1^2}{z_\alpha^2} + \frac{\Omega_1^2}{(\omega^2 - \Omega_1^2)} \frac{\left( \frac{J_1^2}{z_\alpha^2} + J_1'^2 - 2 \frac{\omega J_1 J_1'}{\Omega_1 z_\alpha} \right)}{\left( 1 + \frac{\rho_2}{\rho_1} \right)} \right. \right. \\
& \left. \left. + \frac{\omega_{p2}^2}{\omega_{p1}^2} \frac{\Omega_1^2}{(\omega^2 - \Omega_2^2)} \frac{\left( \frac{J_1^2}{z_\alpha^2} + J_1'^2 - 2 \frac{\omega J_1 J_1'}{\Omega_2 z_\alpha} \right)}{\left( 1 + \frac{\rho_2}{\rho_1} \right)} + N_\parallel^2 \left( \frac{J_1^2}{z_\alpha^2} + J_1'^2 \right) \right] \right\}, \tag{20}
\end{aligned}$$

where  $N_\perp^2 = c_A^2 k_\perp^2 / \omega^2$ .

The dispersion relation given in Eq. (20) is symmetric in the two ion species, subscripts 1 and 2, as it must be since they have been treated on an exactly equal footing. As already mentioned, we shall concentrate on the case where species 1 and 2 are present in comparable proportions and will treat the case of equal proportions when we come to a discussion of the solutions of Eq. (20).

Although Eq. (20) appears rather complicated its content can be readily appreciated. The left-hand-side of the equation describes the fast Alfvén wave, the first bracket, and the ion hybrid wave, the second bracket. These two waves may couple when  $c_A k_\perp \approx \Omega_{ii}$  and this can be seen most easily for  $N_\parallel = 0$ . However, the coupling is not restricted to this special case but can occur over a significant range of parallel wave numbers when the two-ion species are present in comparable concentrations. However, we shall not be concerned with this coupling in this paper but instead will concentrate on the solutions for the ion hybrid wave for shorter wavelengths away from the coupling region, namely  $k_\perp > \Omega_{ii} / c_A$ .

The right-hand-side of Eq. (20) describes the cyclotron interaction of the superthermal ions (the alpha-particles in this paper) with the ion hybrid wave or with the fast Alfvén wave supported by the two-ion species. The corresponding interaction with the fast wave for a single ion species plasma has been analyzed in Ref. 6. Since the ion hybrid wave is supported by two ion species there are two groups of terms on the right-hand side, corresponding to the interaction of the alpha-particles with each ion species. A further discussion of this point will be given in the next section.

### III. THE STABILITY OF THE ION HYBRID WAVE

In this section a solution for the ion hybrid wave will be obtained treating the influence of the superthermal alpha-particles perturbatively. The perturbation parameter is clearly the ratio of the alpha-particle density to the sum of the densities of the two thermal ion species and is given by the term  $\omega_{p\alpha}^2 / (\omega_{p1}^2 + \omega_{p2}^2)$  in Eq. (20). Before discussing the stability of the ion hybrid wave we remark that although we are justified in neglecting the cyclotron damping of the thermal ions, the finite Larmor radius terms will contribute a small correction to the frequency of the ion hybrid wave. In order to avoid a further significant complication of Eq. (20) we have neglected these terms. However, they are included in the numerical solutions to be presented later. In discussing the significance of the alpha-particle terms on the right-hand-side of Eq. (20) it is still a reasonable approximation to assume  $\omega \approx \Omega_{ii}$  since our analysis is restricted to long wave lengths,  $k_\perp^2 v_{Tj}^2 / \Omega_j^2 \ll 1$  where the subscript ‘‘j’’ refers to the thermal ion species.

Returning to our discussion of the right-hand-side of Eq. (20) we note the following. As already mentioned there are two groups of terms, one for each thermal ion species. In addition, each of these groups can be divided into two further sub-groups, the first is proportional to  $[-1 + (\Omega_\alpha / k_\parallel v_{T\parallel\alpha}) Z(\zeta_{1\alpha})]$  and the second to  $[1 + \zeta_{1\alpha} Z(\zeta_{1\alpha})]$ . The significance of the first sub-group is that it survives when the alpha-particle distribution is isotropic and can produce instability for either sign of  $\zeta_{1\alpha}$ . The second sub-group arises directly from anisotropy and can only produce instability when  $\zeta_{1\alpha} < 0$ , a characteristic of the effect of anisot-

ropy. Applied to the case of an inhomogeneous plasma, the isotropic mechanism can produce instability on both high and low magnetic field sides of the Doppler shifted cyclotron resonance of the superthermal alpha-particles whereas the anisotropic mechanism can only drive an instability on the high field side.

In the case of the isotropic sub-group, the dominant term is  $N_{\perp}^2 R$  where  $N_{\perp}^2 > 1$  away from the coupling region with the fast Alfvén wave. For this term to be destabilizing, we require  $R < 0$ . This will occur first between the first maximum of  $J_1$  and its first zero, i.e. the argument  $z_{\alpha}$  of  $J_1$  should be in the range  $1.8 < z_{\alpha} < 3.8$ . Choosing  $z_{\alpha} \approx 3$  as a representative value and putting  $k_{\perp} = x \Omega_{ii}/c_A$ , where  $x > 1$ , we obtain

$$\frac{v_{\perp 0}}{c_A} = \frac{3\Omega_{\alpha}}{x\Omega_{ii}}. \quad (21)$$

Hence, the shorter the perpendicular wavelength of the ion hybrid wave the larger the value of  $x$  and the smaller the

value of  $v_{\perp 0}/c_A$  required for instability. Evidently, instability can occur for sub-Alfvénic alpha-particles even for an isotropic distribution, e.g. a shell distribution. This conclusion is not surprising since the ion hybrid wave is a slow wave becoming progressively slower as  $k_{\perp}$  increases. The second and third terms of this sub-group tend to cancel since  $(\Omega_{ii}^2 - \Omega_1^2)$  and  $(\Omega_{ii}^2 - \Omega_2^2)$  are necessarily of different signs. The term  $N_{\parallel}^2(R+P)$  is less important than the first since  $N_{\parallel}^2 \ll 1$ . By the same reasoning the dominant term from the anisotropic group is the first term  $N_{\perp}^2 J_1^2/z_{\alpha}^2$ .

Let us now obtain the condition for instability of the ion hybrid wave. The above arguments indicate that the most unstable conditions occur when, (a)  $\zeta_{1\alpha} \approx -1$  and (b)  $1.8 < z_{\alpha} < 3.8$ , say  $z_{\alpha} \approx 3$ . We shall restrict the present analysis to long wavelengths  $k_{\perp}^2 \rho_j^2 \ll 1$ , where  $\rho_j^2 = v_{Tj}^2/\Omega_j^2$ , and  $N_{\parallel}^2 \ll 1$  in order to minimize the collisionless electron damping. Under these circumstances we can assume  $\omega \approx \Omega_{ii}$  on the right-hand-side of Eq. (20) and look for a solution  $\omega = \Omega_{ii} + \delta\omega$ . Substituting this into Eq. (20) and solving for  $\text{Im}(\delta\omega)$  we obtain

$$\begin{aligned} \text{Im}(\delta\omega) \approx & \frac{\omega_{p\alpha}^2}{(\omega_{p1}^2 + \omega_{p2}^2)} \frac{(\Omega_{ii}^2 - \Omega_1^2)(\Omega_{ii}^2 - \Omega_2^2)}{2\Omega_{ii}(c_A^2 k_{\perp}^2 - \Omega_{ii}^2)} \left\{ \frac{\Omega_{\alpha}}{k_{\parallel} v_{T\parallel\alpha}} \left[ N_{\perp}^2 R + \frac{\Omega_1^2}{(\Omega_{ii}^2 - \Omega_1^2)} \frac{\left( R + P - 2 \frac{\Omega_{ii}}{\Omega_1} Q \right)}{\left( 1 + \frac{\rho_2}{\rho_1} \right)} \right. \right. \\ & + \frac{\omega_{p2}^2}{\omega_{p1}^2} \frac{\Omega_1^2}{(\Omega_{ii}^2 - \Omega_2^2)} \frac{\left( R + P - 2 \frac{\Omega_{ii}}{\Omega_2} Q \right)}{\left( 1 + \frac{\rho_2}{\rho_1} \right)} + N_{\parallel}^2 (R + P) \left. \right] + 2\zeta_{1\alpha} \frac{v_{\perp 0}^2}{v_{T\parallel\alpha}^2} \left[ N_{\perp}^2 \frac{J_1^2}{z_{\alpha}^2} + \frac{\Omega_1^2 \left( J_1^2 + z_{\alpha}^2 J_1'^2 - 2 \frac{\Omega_{ii}}{\Omega_1} z_{\alpha} J_1 J_1' \right)}{z_{\alpha}^2 (\Omega_{ii}^2 - \Omega_1^2) \left( 1 + \frac{\rho_2}{\rho_1} \right)} \right. \\ & \left. \left. + \frac{\omega_{p2}^2}{\omega_{p1}^2} \frac{\Omega_1^2}{(\Omega_{ii}^2 - \Omega_2^2)} \frac{\left( J_1^2 + z_{\alpha}^2 J_1'^2 - 2 \frac{\Omega_{ii}}{\Omega_2} z_{\alpha} J_1 J_1' \right)}{z_{\alpha}^2 \left( 1 + \frac{\rho_2}{\rho_1} \right)} + N_{\parallel}^2 \left( \frac{J_1^2}{z_{\alpha}^2} + J_1'^2 \right) \right] \right\} \pi^{1/2} \exp(-\zeta_{1\alpha}^2). \quad (22) \end{aligned}$$

This expression can be greatly simplified for a specific case such as a deuterium-tritium plasma with equal concentrations. Under these conditions, Eq. (22) reduces to the following expression for the bare growth rate:

$$\begin{aligned} \frac{\gamma_0}{\Omega_{ii}} \equiv \text{Im} \left( \frac{\delta\omega}{\Omega_{ii}} \right) = & - \frac{(n_{\alpha}/n_D)}{10(N_{\perp}^2 - 1)} \left\{ \frac{\Omega_{\alpha}}{k_{\parallel} v_{T\parallel\alpha}} \left[ N_{\perp}^2 R - \frac{6}{5} \frac{\sqrt{2}}{\sqrt{3}} Q + N_{\parallel}^2 (R + P) \right] + 2\zeta_{1\alpha} \frac{v_{\perp 0}^2}{v_{T\parallel\alpha}^2} \right. \\ & \left. \times \left[ N_{\perp}^2 \frac{J_1^2}{z_{\alpha}^2} - \frac{6}{5} \frac{\sqrt{2}}{\sqrt{3}} \frac{J_1 J_1'}{z_{\alpha}} + N_{\parallel}^2 \left( \frac{J_1^2}{z_{\alpha}^2} + J_1'^2 \right) \right] \right\} \pi^{1/2} \exp(-\zeta_{1\alpha}^2). \quad (23) \end{aligned}$$

It is clear that  $\gamma_0 > 0$  for  $z_{\alpha} \approx 3$  and  $\zeta_{1\alpha} \approx -1$ . For instability to occur the growth rate, given by Eqs. (22) or (23) must exceed the damping rate of the electrons. The electron damping rate of the ion hybrid wave has been derived previously,<sup>2</sup> and for a D-T plasma with equal concentrations, is given approximately by

$$\text{Im}(\delta\omega)_e \approx \frac{6}{50} \left( \frac{\Omega_D^2}{\omega_{pD}^2} \right)^2 \frac{(\omega^2 - \Omega_D^2)(\omega^2 - \Omega_T^2)}{\omega \Omega_{ii}^2} \frac{\omega^2}{\Omega_D^2} \frac{n_{\parallel}^2 n_{\perp}^4}{(N_{\perp}^2 - 1)} \frac{k_{\perp}^2 v_{Te}^2}{2\omega_{pe}^2} \frac{\pi^{1/2} \zeta_e \exp(-\zeta_e^2)}{|1 + \zeta_e Z(\zeta_e)|^2}, \quad (24)$$

where  $\zeta_e = \omega / (k_{\parallel} v_{Te})$ . In the Figs. 2, 5(a), 5(b), and 6 below we have further simplified this expression by replacing  $\omega$  with  $\Omega_{ii}$ , consistent with the perturbative nature of these approximations.

#### IV. NUMERICAL SOLUTIONS OF THE GENERAL DISPERSION RELATION

In this section we present solutions of the full electromagnetic dispersion relation, Eq. (1), for a deuterium-tritium plasma containing a small population of alpha-particles having the distribution given by Eq. (12). The results presented are for equal concentrations of deuterium and tritium ions. We assume that the deuterium and tritium ions and the electrons have Maxwellian distributions. Unstable solutions of the full dispersion relation were sought for the conditions obtained from the analysis of the reduced dispersion relation. We present results typical of both the core and edge plasmas of TFTR. The first set are relevant to the alpha-channelling mechanism and the second to ion cyclotron emission from the edge plasma. The parameters appropriate to the core are taken to be  $B_0 = 4.9$  T,  $n_e = 7 \times 10^{19} \text{ m}^{-3}$ ,  $T_e = 10$  keV,  $T_D = T_T = 20$  keV with an alpha particle density  $n_{\alpha} = 0.01 n_e$ . The densities of deuterium and tritium are, of course,  $n_D = n_T = 0.49 n_e$ . The parameters assumed for the edge region are  $B_0 = 3.62$  T,  $n_e = 1.5 \times 10^{19} \text{ m}^{-3}$ ,  $T_e = 1$  keV,  $T_D = T_T = 3.5$  keV,  $n_{\alpha} = 0.0001 n_e$  with  $n_D = n_T$ . The parameters for the alpha-particle distribution (12) are specified as  $T_{\perp\alpha}, T_{\parallel\alpha}$  and  $v_d$  where  $T_{\perp\alpha} = \frac{1}{2} m_{\alpha} v_{\perp 0}^2$  and  $T_{\parallel\alpha} = \frac{1}{4} m_{\alpha} v_{\parallel \alpha}^2$ . [Notice that  $\langle v_{\parallel}^2 \rangle_{\alpha} = \frac{1}{2} v_{\parallel \alpha}^2$  for the distribution (12).] In all of the numerical results presented here,  $v_d = 0$ , and we have held  $T_{\perp\alpha} + T_{\parallel\alpha} = 3.5$  MeV, consistent with our desire to simulate fusion-born alpha-particles.

In Fig. 1(a) we show dispersion curves of the ion hybrid wave driven unstable by the alpha-particles for core parameters with  $T_{\parallel\alpha} = 2$  MeV and  $T_{\perp\alpha} = 1.5$  MeV. The real part of the frequency of the ion hybrid wave as a function of  $k_{\perp}$  is plotted for five different values of parallel wavelength, indicated in meters in insets to the figure. In Fig. 1(b) we show the growth rates of these five waves. As the ion hybrid wave approaches cut-off with decreasing  $k_{\perp}$ , near the two-ion hybrid frequency (30.5 MHz, here), it smoothly connects with the fast Alfvén wave and plunges toward zero frequency. (We have not analyzed this connection in the present paper, and our approximations are not applicable to the fast wave.) Growth is clearly confined to the ion hybrid wave.

The computed results shown in Fig. 1(b) confirm the prediction that  $z_{\alpha} \approx 3$  for instability, as discussed in Sec. III. For the core parameters of Figs. 1(a) and 1(b),  $z_{\alpha} \approx 3$  at  $k_{\perp} / 2\pi = 0.13 \text{ cm}^{-1}$ , very near the maximum growth rate observed for the different values of  $\lambda_{\parallel}$  studied. The dependence of the growth rate on  $k_{\parallel}$  is governed by the alpha-particle (or hot ion) cyclotron resonance condition. The requirement can be written (approximately) as  $-2 < \zeta_{1\alpha} < 0$ . This guarantees that both terms in Eq. (23) are positive and that there is a significant number of resonant alpha-particles. This is illustrated by Figs. 1(a) and 1(b) where the maximum growth rates obtained for various values of  $\lambda_{\parallel}$  from 0.5 m to 3.3 m correspond (approximately) to values of  $\zeta_{1\alpha}$  of  $-0.3$  and  $-2$ ,

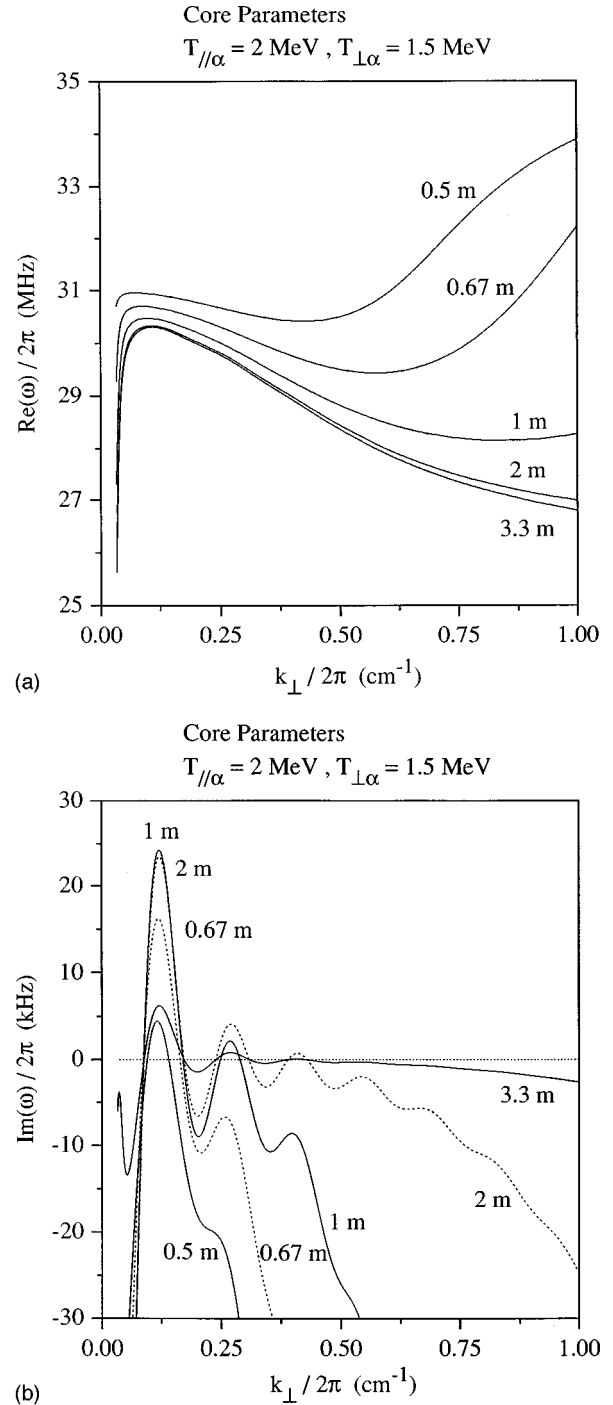


FIG. 1. (a)  $\text{Re}(\omega)$  and (b)  $\text{Im}(\omega)$  versus  $k_{\perp}$  for parameters typical of the core plasma at TFTR, given in the text, the indicated alpha-particle temperatures and parallel wavelengths  $\lambda_{\parallel} = 3.3, 2, 1, 0.67$  and  $0.5$  m. In (b) dashed lines are used for every other parallel wavelength for clarity and a horizontal dotted line indicates zero growth rate.

respectively. The variation of the growth rate with  $\lambda_{\parallel}$  clearly shows the existence of an optimum value of  $\lambda_{\parallel}$ .

Instability can only occur, of course, provided that the alpha-particle drive exceeds the electron Landau damping. The dependence of the electron Landau damping on the various parameters is very well described by Eq. (24). The first point to note is that the damping is weak provided  $N_{\perp}$  is not



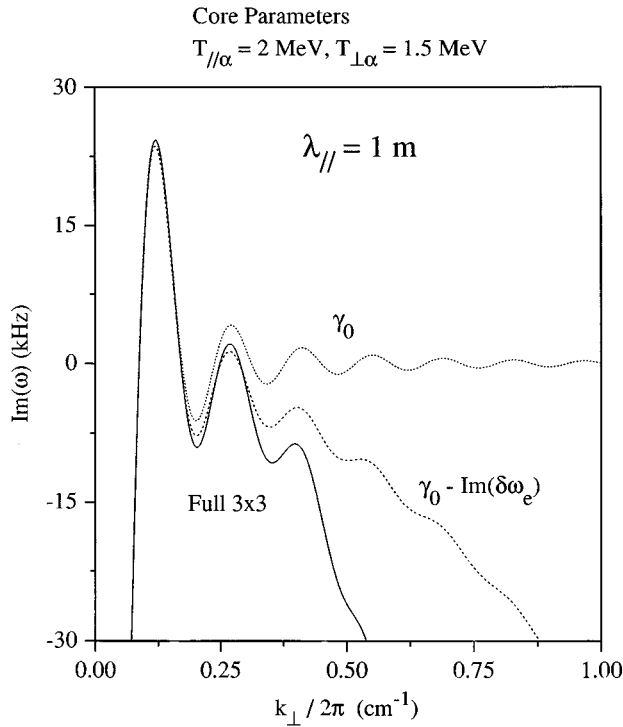


FIG. 2. A comparison of the analytic predictions with the full numerical solution: the bare growth rate, Eq. (23) (dotted), the bare growth rate corrected by the electron Landau damping decrement given by Eq. (24), (dashed) and the growth rate given by Eq. (1) ("Full 3×3," solid) versus  $k_{\perp}$  for the parameters of Fig. 1 and  $\lambda_{\parallel}=1$  m.

large, regardless of the value of  $\zeta_e$ , the ratio of the parallel phase speed to the electron thermal velocity. The weak electron Landau damping is due to the factor  $k_{\parallel}^2 v_{Te}^2 / \omega_{pe}^2$  which is of the order  $10^{-7}$  for parallel wavelengths of about a meter. It should also be emphasized that Eqs. (23) and (24) apply to the case where  $N_{\perp} > 1$ . It can be seen that the electron Landau damping reaches a minimum value when  $N_{\perp} = 2$ . The optimum value of  $N_{\perp}$  for instability, corresponding to  $z_{\alpha} \approx 3$ , gives a values of  $N_{\perp} \approx 3.5$  for the parameters of Fig. 1.

By a straightforward extension of the arguments in Sec. III it is anticipated that more than one interval of instability may be observed with increasing  $k_{\perp}$ , though with progressively smaller growth rates. For the core parameters the 2 m, parallel wavelength is unstable on three such intervals, as shown in Fig. 1(b). However, as Eq. (24) shows, the damping increases with  $N_{\perp}^2$  and eventually becomes strong enough to prevent further unstable intervals.

Both sets of curves in Figs. 1(a) and 1(b) were obtained by solving the complete dispersion equation (1) numerically. In Fig. 2 we compare this solution to our approximations, Eqs. (23) and (24), for the case of fastest growth. [Re( $\omega$ ) is set equal to  $\Omega_{ii}$  in these equations for the calculations in this section.] The bare growth rate,  $\gamma_0$ , alone predicts instability in several intervals on the  $k_{\perp}$ -axis; however these higher- $k_{\perp}$  bands are stabilized by electron Landau damping, and the bare growth rate corrected with the approximate electron damping decrement, Eq. (24), agrees well with the exact result in this regard. The corrected growth rate gives an excel-

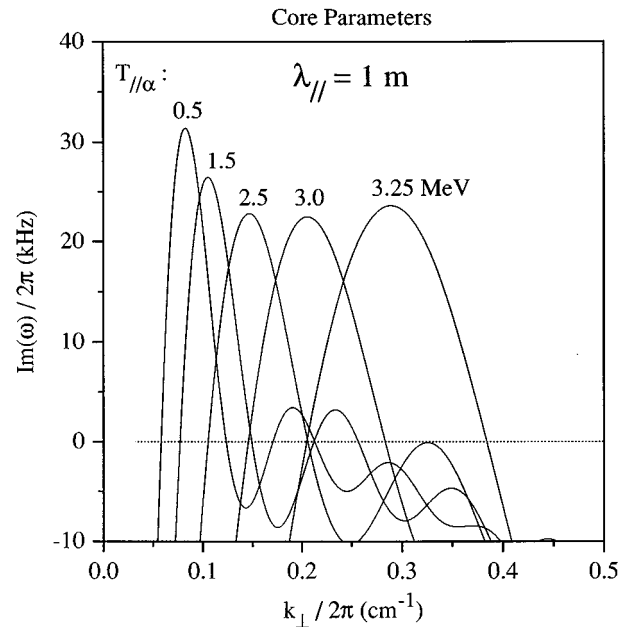


FIG. 3. The growth rate of the ion hybrid wave at  $\lambda_{\parallel}=1$  m according to Eq. (1) versus  $k_{\perp}$  for the parameters of Figs. 1 and 2 but for different choices of the alpha-particle temperatures, as indicated, with  $T_{\perp\alpha}=3.5$  MeV  $-T_{\parallel\alpha}$  enforced. A dotted line indicates zero growth rate.

lent approximation to the threshold for growth in this case (damping by deuterium and tritium is ignorable), and is invaluable for providing a global picture of the instability (see Fig. 6 below).

In Fig. 3 we summarize the behavior of the instability as a function of  $T_{\parallel\alpha}$  ( $=3.5$  MeV  $-T_{\perp\alpha}$ ) for the core parameters using the 1 m parallel wave length, approximately the fastest growing wave in the core plasma. As expected, the range of unstable frequencies is significantly broadened as  $T_{\parallel\alpha}$  increases. Another noteworthy point concerns the ratio  $v_{\perp\alpha}/c_A$  for the unstable waves. For the core parameters studied, this ratio varies from 0.42 ( $T_{\perp\alpha}=0.25$  MeV) to 1.04 ( $T_{\perp\alpha}=3$  MeV), and for the edge parameters from 0.27 to 0.66 for the same alpha-particle temperatures. Thus, except near the coupling region with the fast wave, the ion hybrid wave is sub-Alfvénic which, as already mentioned, is to be expected since the ion hybrid wave is a slow wave which has in general no connection with the Alfvén speed. It is also worth noting that  $(k_{\perp}\rho_D)^2$  varies from 0.04 to 0.4 at maximum growth rate for the core parameters as  $T_{\perp\alpha}$  changes from 3 MeV to 0.25 MeV; lower values of  $T_{\perp\alpha}$  require higher values of  $k_{\perp}$  to maintain the instability criterion  $z_{\alpha} \approx 3$ . For the edge plasma the corresponding range of  $(k_{\perp}\rho_D)^2$  is 0.01 to 0.4 for the fastest growing (2 m) parallel wavelength [see Fig. 4(b)]. Hence the small Larmor radius assumption used to derive the analytic results is reasonably well satisfied by the fastest growing waves.

Notice that in Fig. 1(a) waves with shorter parallel wave lengths approach the deuterium cyclotron frequency (37.4 MHz, here) with increasing  $k_{\perp}$ , whereas those with longer parallel wavelengths approach the tritium cyclotron frequency (24.9 MHz). It is tempting to conjecture that by tuning the parallel wavelength it may be possible to preferen-

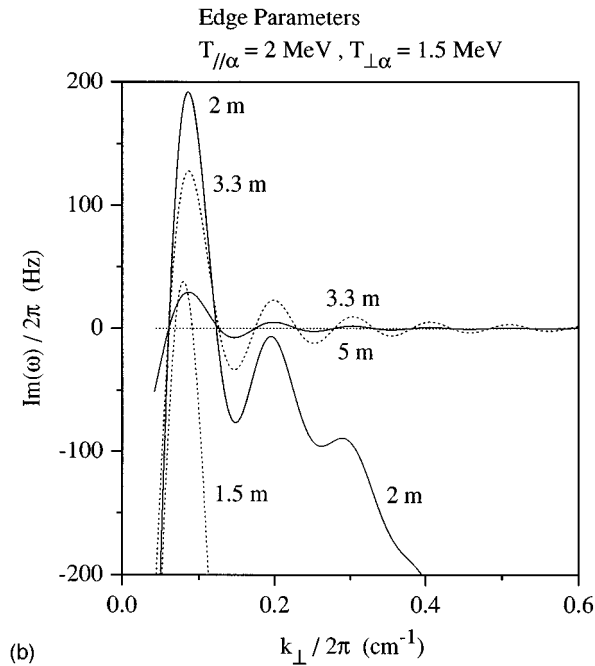
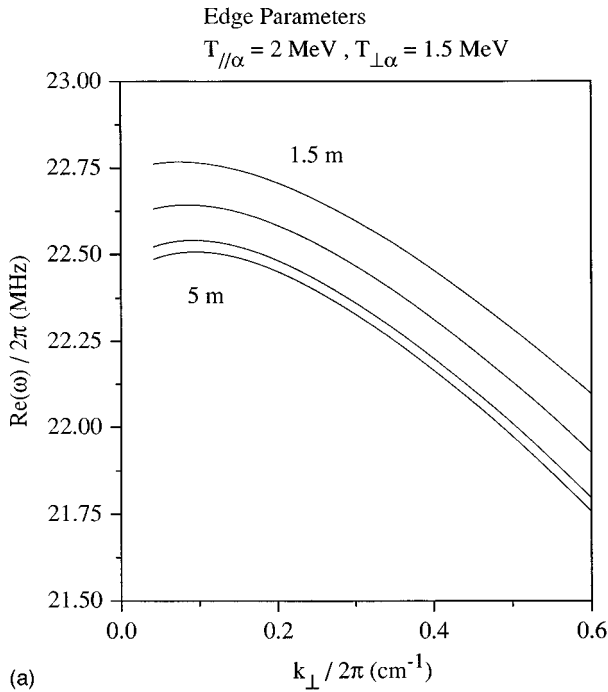


FIG. 4. (a)  $\text{Re}(\omega)$  and (b)  $\text{Im}(\omega)$  versus  $k_{\perp}$  for parameters typical of the edge plasma at TFTR, given in the text, the indicated alpha-particle temperatures and parallel wavelengths  $\lambda_{\parallel} = 5, 3.3, 2$  and  $1.5$  ms. In (b) dashed lines are used for every other parallel wavelength for clarity and a horizontal dotted line indicates zero growth rate.

tially heat one or the other majority ion species via cyclotron damping at the fundamental in an inhomogeneous plasma.

For the edge parameters we find many more bands of instability in  $k_{\perp}$ -space due to the smaller electron temperature assumed in this case. Dispersion curves and growth rates are shown for four different parallel wavelengths in Figs. 4(a) and 4(b), for the same alpha-particle temperatures used in Fig. 1. The growth rate is reduced by roughly a factor of

100 from the core-parameter values, consistent with the reduction in  $n_{\alpha}$ .

Notice that the maximum growth rate is achieved for longer parallel wavelengths at the edge than in the core, consistent with the requirement, discussed above, that  $(\omega - \Omega_{\alpha})/k_{\parallel}v_{T\parallel\alpha} \approx -1$ , imposed here for the lower magnetic field strength of the edge plasma. The cooler electron temperature of the background edge plasma allows more bands of instability to emerge at the longer parallel wavelengths, compared to the core plasma, and we discover six or more bands of instability along the  $k_{\perp}$ -axis for parallel wavelengths greater than about 3 m, though the growth rates in the higher-order bands are much reduced from the peak growth rate in the primary band. Our approximate growth rate,  $\gamma_0 - \text{Im}(\delta\omega_e)$ , is again in very good agreement with the growth rate obtained by solving Eq. (1) in regions of instability and gives excellent approximations to the locations of threshold values of  $k_{\perp}$  [see Figs. 5(a) and 5(b)]. In Figs. 6(a) and 6(b) we have plotted the approximate growth rate as contour lines in  $(k_{\perp}, \lambda_{\parallel})$ -space for the edge and core parameters respectively, with  $T_{\perp\alpha} = 1.5 \text{ MeV}$  and  $T_{\parallel\alpha} = 2 \text{ MeV}$  and  $\lambda_{\parallel} = 2\pi/k_{\parallel}$ . Upper-most contour levels were chosen near the maximum growth rate value in each case, with successive lower levels reduced by a factor of 10 from the previous level. The maximum growth rate occurs within the innermost contour in the lower left corner of each figure. The higher-band unstable regions are only very weakly unstable; the spectrum of unstable waves is clearly dominated by waves with parallel wavelengths of 1 (core) or 2 (edge) meters and perpendicular wavelengths of about 10 cm, for this choice of alpha-particle temperatures.

We calculated relaxation rates<sup>13</sup> for 3.5 MeV alpha-particles in deuterium and in tritium for the core and edge parameters used in this paper. For the core parameters we find the rate of alpha-particle collisional energy relaxation to be  $0.096 \text{ s}^{-1}$  in deuterium and  $0.064 \text{ s}^{-1}$  in tritium. For the edge parameters the rate of energy relaxation is  $0.021 \text{ s}^{-1}$  in deuterium and  $0.014 \text{ s}^{-1}$  in tritium. (Energy relaxation rates dominate slowing-down and parallel and perpendicular diffusion rates in all cases.) Maximum growth rates for each set of parameters studied here are well above these values, however the feeble rates, particularly near the threshold, may not be observable. The relaxation rates should serve as effective lower bounds for the growth rates presented here; for example, in Fig. 6(a) the lowest contour level is at  $0.1 \text{ s}^{-1}$ , about five times larger than the alpha-particle energy relaxation rate for the edge parameters.

To generate our numerical results we solve the full dispersion relation by Newton-Raphson iteration in the complex- $\omega$  plane using a tolerance of error that is adjusted until a certain accuracy criterion is met at each candidate root. Equation (1) results from equating to zero the determinant of the coefficient matrix of the well-known eigenvalue equation for the components of the wave electric field  $\mathbf{E}$ . We write the eigenvalue equation in the form

$$[\eta^2(\hat{\mathbf{k}}\hat{\mathbf{k}} - \mathbf{I}) + \mathbf{I} + \chi] \cdot \mathbf{E}(\mathbf{k}, \omega(\mathbf{k})) = 0. \quad (25)$$

The susceptibility tensor is defined by<sup>10</sup>

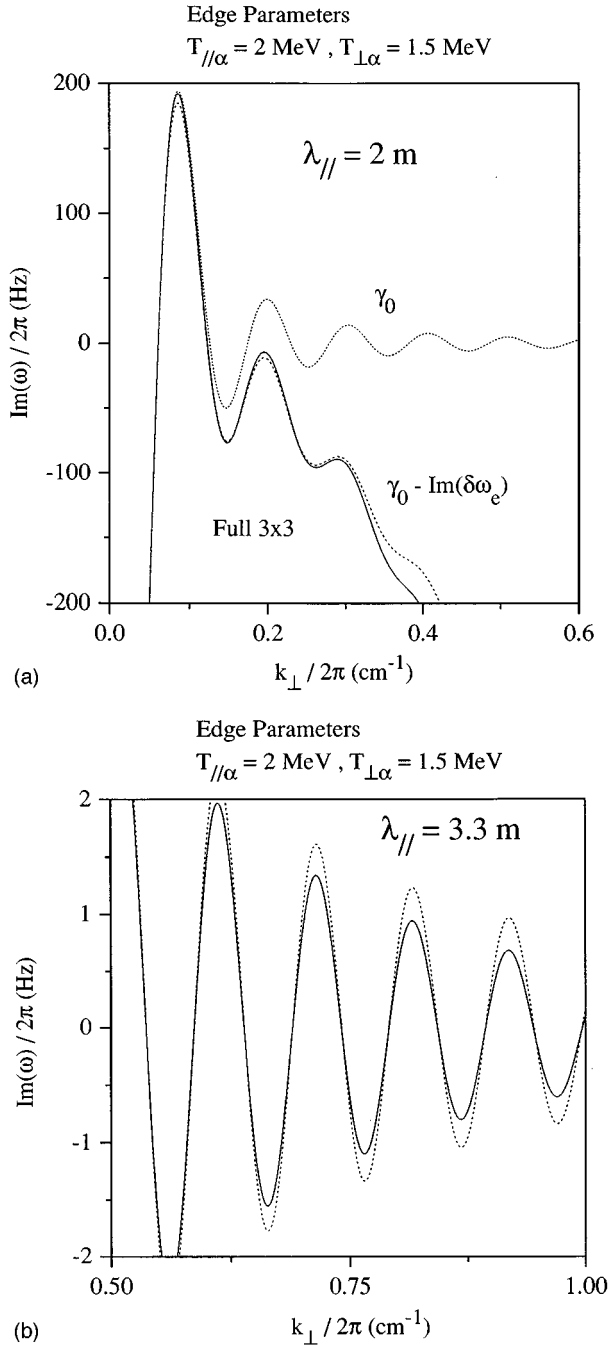


FIG. 5. (a) A comparison of the analytic predictions with the full numerical solution, as in Fig. 2 but for the edge parameters of Fig. 4 and  $\lambda_{\parallel}=2 \text{ m}$ . (b) A similar comparison as in (a) but here for  $\lambda_{\parallel}=3.3 \text{ m}$  and at higher values of  $k_{\perp}$ . The full solution (solid) and the analytic approximation,  $\gamma_0 - \text{Im}(\delta\omega_e)$  (dashed), are plotted; the bare growth rate is not shown.

$$\varepsilon = \mathbf{I} + \chi,$$

where  $\mathbf{I}$  is the unit dyadic. Notice that all quantities appearing in Eq. (25), except  $\mathbf{k}$ , are complex, including  $\eta \equiv kc / \omega(\mathbf{k})$ .

From the dispersion equation (25) it follows directly<sup>14</sup> that

$$\frac{\text{Im}(\omega(\mathbf{k})\mathbf{E}^+ \cdot \chi \cdot \mathbf{E})}{[|\eta|^2|\mathbf{E}_T|^2 + |\mathbf{E}|^2]} = -\text{Im}(\omega(\mathbf{k})), \quad (26)$$

### Contours of Constant Growth Rate

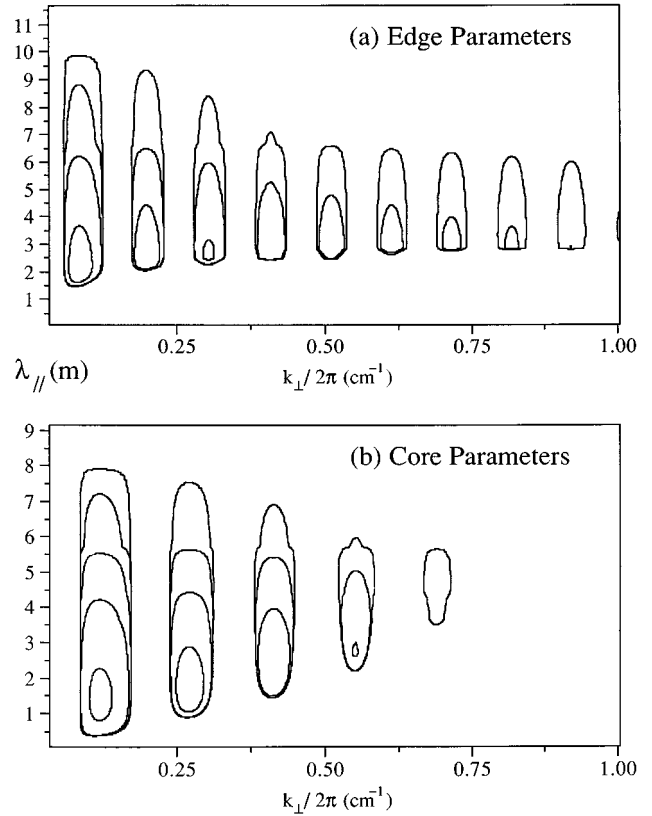


FIG. 6. Contours of constant growth rate,  $\gamma_0 - \text{Im}(\delta\omega_e)$ , according to our analytic approximations for edge (a) and core (b) parameters with  $T_{\perp\alpha}=1.5 \text{ MeV}$  and  $T_{\parallel\alpha}=2 \text{ MeV}$ . In (a) contour levels are at 100, 10, 1 and 0.1 Hz and in (b) contour levels are at 20, 2, 0.2, 0.02 and 0.002 kHz. The maximum growth rate is reached inside the small oval in the lower left corner in each case.

which expresses the conservation of the sum of the electromagnetic field energy density of the wave and the total particle kinetic energy density. ( $\mathbf{E}_T$  denotes the transverse part of the electric field and  $\mathbf{E}^+$  the Hermitian conjugate.) Our accuracy criterion is defined by insisting that this equation be satisfied to a certain number of significant digits, typically 4.

Writing the susceptibility  $\chi$  as the sum of the susceptibilities of each particle species, we can identify on the left-hand-side of Eq. (26) the sum of the power absorbed by each species. This sum must equal the (negative) growth rate of the wave. The left-hand-side may be further dissected to discover that portion of the power going into irreversible heating of a particular species and that portion associated with that species' participation in the wave motion.<sup>15</sup> Thus, since the ion hybrid wave is supported by the two bulk ion species, we may write

$$\begin{aligned} \text{Im}(\omega\mathbf{E}^+ \cdot \chi^i \cdot \mathbf{E}) &\approx \omega_R \mathbf{E}^+ \cdot \chi_i^i \cdot \mathbf{E} + \text{Im}(\omega) \\ &\times \frac{d}{d\omega} (\omega\mathbf{E}^+ \cdot \chi_R^i \cdot \mathbf{E})_{\omega_R}, \end{aligned} \quad (27)$$

where we have used the fact that  $\gamma \ll \omega_R$  with  $\omega = \omega_R + i\gamma$ .  $\chi_R^i$  and  $\chi_i^i$  are the real and imaginary parts of the bulk ion

susceptibilities, respectively, where the superscript “*i*” denotes deuterium or tritium. With the aid of Eq. (27), Eq. (26) can be written in the form

$$\begin{aligned}
 & -\text{Im}(\omega) \\
 &= \frac{\sum_{\sigma} \omega_R \mathbf{E}^+ \cdot \chi_I^{\sigma} \cdot \mathbf{E}}{\left\{ |\eta|^2 |\mathbf{E}^T|^2 + |\mathbf{E}|^2 + \sum_{\sigma} \frac{d}{d\omega} (\omega \mathbf{E}^+ \cdot \chi_R^{\sigma}(\omega) \cdot \mathbf{E})_{\omega_R} \right\}}, \quad (28)
 \end{aligned}$$

where the third term in the denominator will be recognized as the contribution to the wave energy density of the plasma particles. The summation is over all species but for the present case, as already mentioned, the ion hybrid wave is supported by the two thermal ion species. For comparable concentrations of the two ion species,  $\chi_R^i$  can be approximated by the cold plasma value. The summation in the numerator of Eq. (28) is also over all species. In the instability region the only significant contribution to  $\chi_I^{\sigma}$  comes from the alpha-particles and the electrons. The cyclotron damping of the deuterons and tritons is negligible. However, on examination of Fig. 1, it can be seen that for larger values of  $k_{\perp}$  the ion hybrid wave can be in fundamental cyclotron resonance with either the deuterons or tritons, depending on the value of  $k_{\parallel}$ . Hence, in an inhomogeneous plasma, for conditions of weak electron damping, the ion hybrid wave could eventually transfer some of its energy to the thermal ions.

## V. SUMMARY AND CONCLUSIONS

We have analyzed the stability of the ion hybrid wave in the presence of a low density population of superthermal ions. The specific case where the superthermal ions are taken to be fusion alpha-particles has been considered. Two particular scenarios have been studied. The first is concerned with the core plasma of the tokamak TFTR and is relevant to the question of alpha-channelling in which a wave is required to extract the free energy from the alpha-particles and eventually transfer it to thermal particles, which can be either ions or electrons. This mechanism is required to operate in the immediate post-birth phase before the alpha-particles have slowed down collisionally. A rather simple, non-thermal distribution function has been used for the fusion alpha-particles which enabled an approximate but tractable analytic dispersion relation to be obtained. This proved to be valuable in guiding a full numerical solution of the exact dispersion relation. The alpha-particle distribution function consisted of a ring distribution for the perpendicular velocity and a Maxwellian for the parallel velocity with a large parallel temperature (of the order of a MeV). The large parallel temperature is essential to enable the alpha-particles to be Doppler shifted into cyclotron resonance with the ion hybrid wave, since the frequency of the ion hybrid wave lies between the cyclotron frequencies of the two-ion species (deuterium and tritium). Under these conditions the ion hybrid wave will not be damped by the thermal ions in the region of

the hybrid resonance. The only damping for frequencies close to the two-ion hybrid frequency is provided by the electrons.

We have demonstrated that the ion hybrid wave can indeed be driven unstable by the immediate, post-birth alpha-particles. This instability is relevant to the alpha-channelling proposed of Fisch *et al.*<sup>5,6</sup> However, the instability mechanism discussed in this paper is complementary to the scheme proposed by Fisch *et al.*<sup>5</sup> The radial inhomogeneity of the alpha-particle distribution is a crucial ingredient of the Fisch alpha-channelling mechanism since the alpha-particles are displaced radially outwards as they exchange energy with the ion hybrid wave. The instability mechanism discussed in the present work is a local effect which relies on the population inversion in velocity space of the alphas at birth and does not require radial inhomogeneity. The role of radial inhomogeneity will enter through its effect on the local resonance conditions of the ion hybrid wave which govern which plasma species interact with the wave.

Since we have restricted our attention to a local model and the case of equal concentrations of deuterium and tritium, we have not addressed the question of whether such an amplified wave might eventually damp on the thermal ions. For the alpha-channelling application a launched wave would evidently be more effective than a spontaneously excited one since it could operate at larger amplitude and thus transfer the alpha-particle energy at a faster rate. The present calculation provides some guidance on the conditions required to amplify a launched wave or just to ensure that energy flows from the alpha-particles to the wave even if, overall, the wave is damped. An advantage of the use of a launched wave is that the latter requirement would be sufficient.

The other situation to which the present calculation may be relevant is that of ion cyclotron emission from the edge region of a tokamak. The alpha-particle distribution function that we have used has been shown to be relevant to ion cyclotron emission from fusion products in the edge plasmas of both JET<sup>7</sup> and TFTR.<sup>8</sup> The instability associated with the fast wave<sup>7</sup> (the magnetoacoustic cyclotron instability) has been identified as the probable ICE mechanism in JET and TFTR.<sup>7,8,16</sup> It is stronger in the JET discharges where the birth speeds of the alpha-particles are super-Alfvénic but it is also relevant for TFTR where the alpha-particles are usually sub-Alfvénic at the edge. This was strikingly demonstrated by the stronger ICE signal at the fundamental cyclotron frequency of the alpha-particles in the low-confinement-mode (L-mode) TFTR discharges<sup>17</sup> for which the alpha-particles are super-Alfvénic. The time evolution of the ICE amplitude has also been modelled successfully in terms of the linear growth rate of the fast wave instability for TFTR.<sup>18</sup> Nevertheless, the particular feature of the present calculation which might be of interest to TFTR is the insensitivity of the ion hybrid wave to the ratio  $v_{\perp 0}/c_A$ . Instability has been obtained for values of this quantity as low as 0.27 and even lower values would be expected to give rise to instability simply by increasing the perpendicular wave number of the ion hybrid wave. Unlike the fast Alfvén wave, increase of the perpendicular wave number produces only a small change in

the wave frequency so that the resonance condition is not greatly altered.

The ion hybrid wave could only give rise to ion cyclotron emission at one frequency and not at cyclotron harmonics without invoking non-linear effects. However, harmonic emission could arise through a similar mechanism to the one analyzed in this paper in which short wavelength ion Bernstein waves are driven unstable by the superthermal alpha-particles. An analysis of this case will be described in a subsequent publication.

It should be noted that the model of a deuterium-tritium plasma with approximately equal concentrations is not the most appropriate one for the edge region which is usually dominated by the influx of deuterium ions from the wall. We have included this case simply to illustrate that the mechanism discussed in this paper might also be of interest for the edge region.

### ACKNOWLEDGMENTS

This work was partly supported by the UK Department of Trade and Industry and EURATOM, by U.S. Department of Energy Grant No. DE-FG02-88ER53263 and by North Atlantic Treaty Organization Collaborative Research Grant No. 920669.

<sup>1</sup>S. J. Buchsbaum, *Phys. Fluids* **3**, 418 (1960).

<sup>2</sup>C. N. Lashmore-Davies, V. Fuchs, A. K. Ram, and A. Bers, "Enhanced coupling of the fast wave to electrons through mode conversion to the ion hybrid wave," submitted to *Phys. Plasmas*.

<sup>3</sup>R. Majeski, C. K. Phillips, and J. R. Wilson, *Phys. Rev. Lett.* **73**, 2204 (1994).

<sup>4</sup>K. M. Young, M. Bell, W. R. Blanchard, N. Bretz, J. Cecchi, J. Coonrod, S. Davis, H. F. Dylla, P. C. Efthimion, R. Fonck, R. Goldston, D. J. Grove, R. J. Hawryluk, H. Hendel, K. W. Hill, J. Isaacson, L. C. Johnson, R. Kaita, R. B. Krawchuk, R. Little, M. McCarthy, D. McCune, K. McGuire, D. Meade, S. S. Medley, D. Mikkleson, D. Mueller, E. Nieschmidt, D. K. Owens, A. Ramsey, A. L. Roquemore, L. Samuelson, N. Sauthoff, J. Schivell, J. A. Schmidt, S. Sesnic, J. Sinnis, J. Strachan, G. D. Tait, G. Taylor, F. Tenney, and M. Ulrickson, *Plasma Phys. Controlled Fusion* **26**, 11 (1984).

<sup>5</sup>N. J. Fisch, *Phys. Plasmas* **2**, 2375 (1995).

<sup>6</sup>N. J. Fisch and J. M. Rax, *Phys. Rev. Lett.* **69**, 612 (1992).

<sup>7</sup>R. O. Dendy, C. N. Lashmore-Davies, K. G. McClements, and G. A. Cottrell, *Phys. Plasmas* **1**, 1918 (1994).

<sup>8</sup>K. G. McClements, R. O. Dendy, C. N. Lashmore-Davies, S. Cauffman, G. A. Cottrell, and R. Majeski, *Phys. Plasmas* **3**, 543 (1996).

<sup>9</sup>The JET Team, *Nucl. Fusion* **32**, 187 (1992).

<sup>10</sup>C. N. Lashmore-Davies, V. Fuchs, G. Francis, A. K. Ram, A. Bers, and L. Gauthier, *Phys. Fluids* **31**, 1614 (1988).

<sup>11</sup>M. Ono, *Phys. Fluids B* **5**, 241 (1993).

<sup>12</sup>T. H. Stix, *Waves in Plasmas* (American Institute of Physics, New York, 1992), p. 252.

<sup>13</sup>D. L. Book, *NRL Plasma Formulary* (Naval Research Laboratory, Washington, DC, 1983), p. 31.

<sup>14</sup>V. D. Shafranov in *Review of Plasma Physics*, edited by M. A. Leontovich (Consultants Bureau, New York, 1967), p. 143.

<sup>15</sup>See Ref. 14, p. 141 and A. Bers, in *Plasma Physics—Les Houches* (Gordon and Breach, New York, 1975), p. 126.

<sup>16</sup>N. Gorelenkov and C. Z. Cheng, *Phys. Plasmas* **2**, 1961 (1995).

<sup>17</sup>S. Cauffman, R. Majeski, K. G. McClements, and R. O. Dendy, *Nucl. Fusion* **35**, 1597 (1995).

<sup>18</sup>R. O. Dendy, K. G. McClements, C. N. Lashmore-Davies, G. A. Cottrell, R. Majeski, and S. Cauffman, *Nucl. Fusion* **35**, 1733 (1995).